32ND INTERNATIONAL COSMIC RAY CONFERENCE, BEIJING 2011

Fermi-LAT study of diffuse gamma-ray emission in the outer Galaxy and implications for Galactic cosmic-rays

T. MIZUNO[1], L. TIBALDO[2], I. GRENIER[3] ON BEHALF OF THE *Fermi* LAT COLLABORATION
[1] *Department of Physical Sciences, Hiroshima University, Higashi-Hiroshima, Hiroshima 739-8526, Japan*
[2] *Dipartimento di Fisica "G. Galilei", Università di Padova, and INFN-Sezione di Padova, Italy*
[3] *Laboratoire AIM, CEA-IRFU/CNRS/Université Paris Diderot, Service d'Astrophysique, CEA Saclay, 91191 Gif sur Yvette, France*
mizuno@hep01.hepl.hiroshima-u.ac.jp
DOI: 10.7529/ICRC2011/V07/0802

Abstract: Galactic diffuse γ-ray emission is a powerful probe to study cosmic rays and the interstellar medium in distant locations. We analyzed the interstellar γ-ray emission from the outer Galaxy measured by the Large Area Telescope (LAT) on board Fermi [1, 2]. The γ-ray emissivity as a function of Galactocentric distance does not show a significant gradient beyond the solar circle, indicating larger cosmic-ray densities than what has been usually assumed so far. We report the analysis and discuss their implications for the origin and propagation of Galactic cosmic rays.

Keywords: cosmic rays – gamma-rays:ISM – ISM:general

1 Introduction

Knowledge of the distribution of cosmic-ray (CR) densities within our Galaxy is a key to understanding their origin and propagation. High-energy CRs interact with the gas in the interstellar medium (ISM) or the interstellar radiation field, and produce γ-rays via nucleon-nucleon interactions, electron Bremsstrahlung and inverse Compton (IC) scattering. Since the ISM is transparent to these γ-rays, we can probe CRs in distant locations of the Galaxy. Although much effort has been made since the COS-B era (e.g., [3, 4, 5]), the results have been limited by the performance of the past instruments. The advent of the *Fermi* Gamma-ray Space Telescope enables studying the spectral and spatial distribution of diffuse γ-rays and CRs with unprecedented sensitivity.

Here we report analyses of diffuse γ-ray emission observed in the second (Galactic longitude $100^\circ \leq l \leq 145^\circ$) and the third ($210^\circ \leq l \leq 250^\circ$) Galactic quadrants. Those windows host kinematically well-defined segments of the Galactic spiral arms present along the line of sight and are the best regions to study the CR density distribution across the outer Galaxy. Although they have been already studied by [6, 7] using EGRET data, the improved sensitivity and angular resolution of the *Fermi* LAT [8] and recent developments in the study of the ISM (e.g., [9, 10, 11, 12]) allow us to examine the CR spectra and density distribution with better accuracy.

2 Data Analysis

Following a well-established approach that dates back to the COS-B era [13], we modeled the γ-ray emission as a linear combination of maps tracing the column density of the interstellar gas. This approach is based on a simple but plausible assumption: γ-rays are generated through interactions of CRs and the interstellar gas, and the ISM itself is transparent to γ-rays. Then, assuming that CR densities do not significantly vary over the scale of the interstellar complexes under study, we can model the γ-ray intensities to first order as a linear combination of contributions from CR interactions with the different gas phases in the various regions along the line of sight.

Then, the γ-ray intensities $I_\gamma(l,b)$ ($\mathrm{s^{-1}\ cm^{-2}\ sr^{-1}\ MeV^{-1}}$) can be modeled as:

$$I_\gamma(l,b) = \sum_i q_{\mathrm{HI},i} \cdot N(\mathrm{H\,I})(l,b)_i + \sum_i q_{\mathrm{CO},i} \cdot W_{\mathrm{CO}}(l,b)_i + q_{\mathrm{EBV}} \cdot \mathrm{E(B\text{-}V)}_{\mathrm{res}}(l,b) + I_{\mathrm{IC}}(l,b) + I_{\mathrm{iso}} + \sum_j \mathrm{PS}_j \ , \quad (1)$$

where the sum over i represents the combination of the Galactic regions, $q_{\mathrm{HI},i}$ ($\mathrm{s^{-1}\ sr^{-1}\ MeV^{-1}}$) and $q_{\mathrm{CO},i}$ ($\mathrm{s^{-1}\ cm^{-2}\ sr^{-1}\ MeV^{-1}\ (K\ km\ s^{-1})^{-1}}$) are the emissivities per H I atom (traced by the 21 cm line of atomic hydrogen) and per W_{CO} unit (as a tracer of molecular gas), respectively. q_{EBV} ($\mathrm{s^{-1}\ cm^{-2}\ sr^{-1}\ MeV^{-1}\ mag^{-1}}$) is the

emissivity per unit of the $E(B-V)_{\rm res}$ map which accounts for the gas not properly traced by H I and CO observations. $I_{\rm IC}$ and $I_{\rm iso}$ are the IC model and isotropic background intensities ($\rm s^{-1}\ cm^{-2}\ sr^{-1}\ MeV^{-1}$), respectively, and $\rm PS_{\it j}$ represents the point source contributions. See [1, 2] for details of the analysis.

3 Results and Discussions

3.1 Emissivity Spectrum and Gradient

In Figure 1 (top panel), we report the emissivity spectra found per H atom in the Local arm, interarm, Perseus arm and outermost regions of the third quadrant assuming spin temperature $T_{\rm S} = 125$ K. For comparison with the local interstellar spectrum (LIS) we also plot the model spectrum used in [14]. We see that the spectral shape of the Local-arm emissivity agrees well with the model for the LIS. The same conclusion can be applied to the measurement of the second quadrant [1].

We also observe that the emissivity spectra do not vary significantly with Galactocentric distances in the outer Galaxy. To examine the spectral shape more quantitatively, we present the emissivity ratios of the interarm and Perseus regions relative to the Local arm in the bottom panels of Figure 1. The ratios are found to be constant except the highest energy bin, which could be affected by the interplay with the outer-arm emissivity (see top panel of Figure 1). We thus conclude that the spectral shapes are consistent with the LIS in the $0.1 - 6$ GeV energy band. Considering that these γ-rays trace CR nuclei of energies from a few GeV to about 100 GeV (e.g., [15]), LAT data indicate that the energy distribution of the main component of Galactic CRs does not vary significantly in the outer Galaxy in the third quadrant.

In Figure 2 we summarize the integrated emissivity gradient (above 200 MeV) found beyond the Solar circle in the second and the third quadrants. We assessed the uncertainties due to the optical depth correction applied to the H I line intensities. The typical statistical error and characteristic systematic error due to the LAT event selection efficiency are $\leq 10\%$ in the energy range under study, and are smaller than the uncertainty due to the optical depth correction. We thus conclude that the most important source of uncertainty in the CR density derivation is currently that in the N(H I) determination. Yet, we can derive robust constraints on the large-scale properties of Galactic CRs, which are discussed below.

3.2 Comparison with a Propagation Model: Implications on Galactic CRs

Despite the uncertainties due to the optical-depth correction, both LAT studies consistently point to a slowly decreasing emissivity profile beyond Galactocentric radius $R = 10$ kpc as shown by Figure 2.

We will consider the predictions by a CR propagation model to see the impact of such a flat profile on the CR source distribution and propagation parameters. We utilize the GALPROP code (see, e.g., [16]), a numerical code which solves the CR transport within the Galaxy. We start from the CR source distribution expresses as

$$f(R) = \left(\frac{R}{R_\odot}\right)^{1.25} \exp\left(-3.56 \cdot \frac{R - R_\odot}{R_\odot}\right) , \quad (2)$$

where $R_\odot = 8.5$ kpc is the distance of the Sun to the Galactic center. As shown in Figure 3, this function is intermediate between the distribution of supernova remnants (SNRs) obtained from the Σ–D relation [17] and that traced by pulsars [18]. We then run the GALPROP code and compare the predicted emissivity distribution (proportional to the density of CRs after propagation) with the LAT measurement. In the calculation, the spatial diffusion coefficient is assumed to be uniform across the Galaxy and is taken as $D_{xx} = \beta D_0 (\rho/4\ {\rm GV})^\delta$, where $\beta \equiv v/c$ is the velocity of the particle relative to the speed of light and ρ is the rigidity. We adopted $D_0 = 5.8 \times 10^{28}\ \rm cm^2\ s^{-1}$ and $\delta = 0.33$ (Kolmogorov spectrum). See [2] for more details of the model calculation. The CR source distribution and propagation model parameters have been used often in the literature (e.g., [19]).

The top panel of Figure 4 compares the calculated profile for the CR halo size of 4 kpc (solid line) with LAT constraints on the third quadrant (bow-tie plot bracketing the profiles obtained for different $T_{\rm S}$). Despite the large uncertainties, LAT data lead to a significantly flatter profile than predicted by our baseline model.

The discrepancy between the γ-ray emissivity gradient and the distribution of putative CR sources has been known as the "gradient problem" since the COS-B era [20]. The most straightforward possibility is a larger halo size ($z_{\rm h}$), as discussed by, e.g., [16, 20, 21]. We therefore tried several choices of $z_{\rm h}$ and D_0 as summarized in the dotted lines in the same figure. The values of $z_{\rm h}$ and D_0 (see the caption of the Figure 4) are chosen to reasonably reproduce the CR measurements at the Earth. A CR source distribution given by equation 2 with a very large halo ($z_{\rm h} \geq 10$ kpc) provides a gradient compatible with the γ-ray data, if we fully take into account the systematic uncertainties.

Considering the large uncertainties in the SNR distribution, a flatter CR source distribution in the outer Galaxy also could be possible. We thus tried a modified CR source distribution, in which the distribution is the same as equation 2 below $R_{\rm bk}$ and constant beyond it (see a thin solid line of Figure 3 as an example). Figure 4 bottom shows the models with several choices of $R_{\rm bk}$ for $z_{\rm h} = 4$ kpc and $D_0 = 5.8 \times 10^{28}\ \rm cm^2\ s^{-1}$. We obtained a reasonable fit to the data using a flat CR source distribution beyond $R = 10$ kpc. Although such a constant CR source density in the outer Galaxy is in contrast with the distribution of SNRs and other tracers of massive star formation (e.g., [22, 23, 24]), a very large halo size and/or a flat CR source distribution seem to be favored by the LAT data.

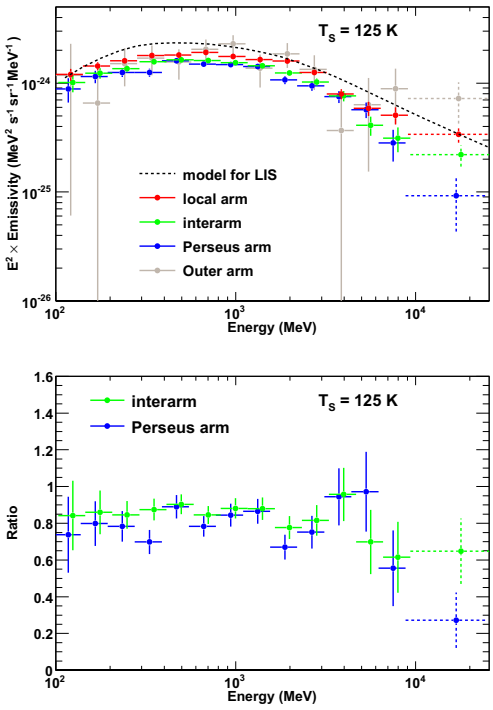

Figure 1: (top) H I emissivity spectra obtained for each region of the third Galactic quadrant compared with the model spectrum for the LIS adopted by [14]. (bottom) The emissivity ratios to that of the Local arm.

Obviously the solution discussed above is not unique. The exploration could be extended to a non-uniform diffusion coefficient (e.g., [25]) or convection (e.g., [26]). An alternative way to reconcile the flat emissivity profile could be to invoke an increase in missing gas mass with Galactocentric distance of the outer Galaxy (e.g., [27, 28]) beyond the local correction applied here. In the future, the extension to the inner part and the accurate determination of the gradient over the whole Galaxy will be key to constraining the CR origin and transport.

The *Fermi* LAT Collaboration acknowledges support from a number of agencies and institutes for both development and the operation of the LAT as well as scientific data analysis. These include NASA and DOE in the United States, CEA/Irfu and IN2P3/CNRS in France, ASI and INFN in Italy, MEXT, KEK, and JAXA in Japan, and the K. A. Wallenberg Foundation, the Swedish Research Council and the National Space Board in Sweden. Additional support from INAF in Italy and CNES in France for science analysis during the operations phase is also gratefully acknowledged.

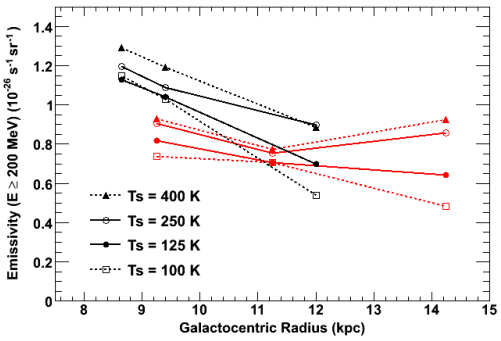

Figure 2: The emissivity per H I atom integrated above 200 MeV as a function of Galactocentric radius for different H I spin temperatures, as measured in the second (black) and the third (red) Galactic quadrants.

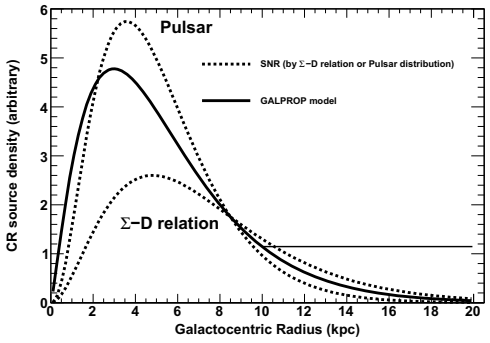

Figure 3: The CR source distribution of our baseline model (solid line), compared with the SNR distribution obtained by [17, 18]. The thin solid line shows an example of the modified distributions introduced to reproduce the emissivity gradient measured by the LAT. (see the bottom panel of Figure 4)

References

[1] Abdo, A. A. et al., ApJ, 2010 **710**: 133
[2] Ackermann, M. et al., ApJ, 2011 **726**: 81
[3] Strong, A. W. et al. A&A, 1988 **207**: 1
[4] Strong, A. W. et al., A&A, 1996 **308**: L21
[5] Bloemen, J. B. G. et al., A&A, 1986 **154**: 25
[6] Digel, S. W. et al, ApJ, 1996 **463**: 609
[7] Digel, S. W. et al., ApJ, 2001 **555**: 12
[8] Atwood, W. B. et al., ApJ, 2009 **697**: 1071
[9] Kalberla, P. M. W. et al., A&A, 2005 **440**: 775
[10] Dame, T. M. et al., ApJ, 2001 **547**: 792
[11] Schlegel, D. J. et al., ApJ, 1998 **500**: 525
[12] Grenier, I. A. et al., Science, 2005 **307**: 1292
[13] Lebrun, F. et al., ApJ, 1983 **274**: 231
[14] Abdo, A. A. et al., ApJ, 2009 **703**: 1249

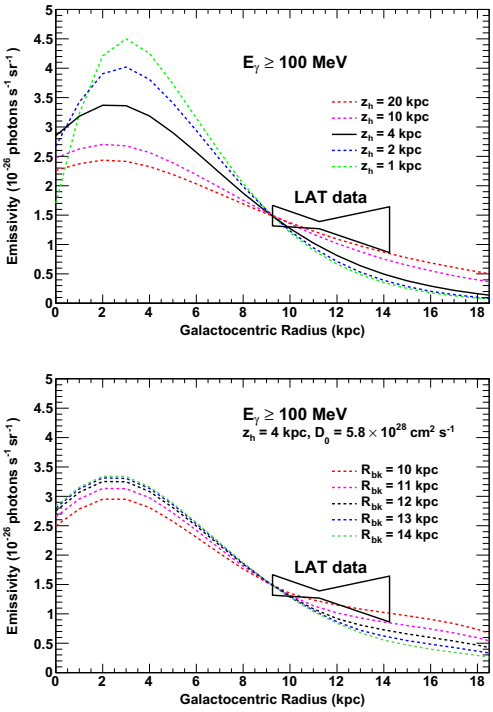

Figure 4: Comparison of the emissivity gradient obtained by the LAT and model expectations using GALPROP. The top panel shows models with different halo sizes and diffusion lengths: $(z_{\rm h}, D_0)$ = (1 kpc, 1.7×10^{28} cm^2 s^{-1}), (2 kpc, 3.2×10^{28} cm^2 s^{-1}), (4 kpc, 5.8×10^{28} cm^2 s^{-1}), (10 kpc, 12×10^{28} cm^2 s^{-1}) and (20 kpc, 18×10^{28} cm^2 s^{-1}). The bottom panel shows different choices of the break distance (from 10 to 14 kpc) beyond which a flat CR source distribution is assumed.

[15] Mori, M. ApJ, 1997 **478**: 225
[16] Strong, A. W. et al, ApJ, 1998 **509**: 212
[17] Case, G. L. et al, ApJ, 1998 **504**: 761
[18] Lorimer, D. R., arXiv:astro-ph/0308501, 2004
[19] Strong, A. W. et al., ApJ, 2004 **613**: 962
[20] Bloemen, H., ARA&A, 1989 **27**: 469
[21] Stecker, F. W. et al, ApJ, 1977 **217**: 843
[22] Ferrière, K. M., Reviews of Modern Physics, 2001 **73**: 1031
[23] Bronfman, L. et al., A&A, 2000 **358**: 521
[24] Diehl, R. et al., Nature, 2006 **439**: 45
[25] Evoli, C. et al., JCAP, 2008 **10**: 18
[26] Breitschwerdt, D. et al., A&A, 2002 **385**: 216
[27] Papadopoulos, P. P. et al, ApJ, 2002 **579**: 270
[28] Wolfire, M. G. et al, ApJ, 2010 **716**: 1191